International Journal of Applied Pharmaceutics

ISSN- 0975-7058 Vol 16, Issue 3, 2024

Original Article

IN SILICO, PREPARATION AND *IN VITRO* STUDIES OF BENZYLIDENE-BASED HYDROXY BENZYL UREA DERIVATIVES AS FREE RADICAL SCAVENGERS IN PARKINSON'S DISEASE

JAGDISH CHAND, AMARJITH THIYYAR KANDY, KAVERI PRASAD, JINU MATHEW, FARHATH SHERIN, GOMATHY SUBRAMANIAN*

Department of Pharmaceutical Chemistry, JSS College of Pharmacy, JSS Academy of Higher Education and Research, Ooty-643001, The Nilgiris, Tamil Nadu, India

***Corresponding author: Gomathy Subramanian; *Email: gomathys@jssuni.edu.in**

Received: 24 Jan 2024, Revised and Accepted: 20 Mar 2024

ABSTRACT

Objective: The study focuses on the benzylidene-based hydroxy benzyl urea derivative as free radical scavengers in PD.

Methods: The derivatives were designed, synthesized, and characterized using FTIR, ^{1}H, ^{13}C-NMR, and Mass spectrometry. Further *in vitro* studies were performed on the SHSY-5Y cell lines. Molecular docking and molecular dynamic studies were performed at 100 ns to predict the binding affinity and stability of the ligand/protein complex.

Results: Among the nine derivatives, compounds HBU-2, and HBU-4were found to have the highest binding affinity-9.699 kcal/mol, and-9.020 kcal/mol with the amino acid interactions SER 149, PHE 157, ARG 158, SER 159, ILE 230, and ASP 231. Further, this HBU-1 to HBU-9 derivatives were produced using a synthesis route. The neurotoxicity studies were performed on the SHSY-5Y cells, where the % cell viability for the compound HBU-2, and HBU-4 was 91.22 %, and 90.42 %at a minimal concentration of 125 µg/ml with a p-value<0.011. Further, the cell counts and LDH assay for the compound HBU-2, and HBU-4 with MPP^{+}treatment predicted 0.72-fold change and 0.66-fold change. The ROS % activity was also measured for compounds HBU-2 and HBU-4 in conjunction with the MPP^{+}induction. In the SHSY-5Y cell line, compound HBU-2 downregulated the ROS level to 45%.

Conclusion: The synthesized compounds were found to have good free radical scavenging properties on SHSY-5Y neuroblastoma cell lines, considering these derivatives could be further assessed using appropriate PD models.

Keywords: Molecular docking, Free radical scavengers, SHSY-5Y neuroblastoma cells, *In vitro*, Parkinson's disease

DOI: https://dx.doi.org/10.22159/ijap.2024v16i3.50628 Journal homepage: https://innovareacademics.in/journals/index.php/ijap

INTRODUCTION

The world's aging population is a global issue that unavoidably contributes to the progressively escalating prevalence rate of neurological disorders [1]. Parkinson's disease (PD), has one of the highest incidence percentiles of all neurodegenerative diseases and is characterized as a motor dysfunction that affects body movement and coordination [2]. PD is currently only managed by symptomatic therapies that do not halt the disease's development. Due to the clinical failures of previously identified drug candidates, there is an urgent need for the development of new and more effective PD treatments [3]. Sirtuin 3 (SIRT3), a well-known mitochondrial deacetylase, is involved in mitochondrial function and metabolism under various stress conditions, resulting in the downregulation of reactive oxygen species (ROS) [4]. SIRT3 is essential for controlling metabolism, autophagy, cell death, inflammatory responses, and ATP generation [5]. In addition, mitochondrial stress, ROS, oxidative stress, proteotoxic stress, and starvation conditions all affect the level of SIRT3. SIRT3 is mostly expressed in metabolically active organs such as the brain, muscle, liver, kidney, and heart and is predominantly found in the mitochondrial nucleus [6, 7]. Additionally, the levels of SIRT3 are impacted by hunger, oxidative stress, mitochondrial stress, and proteotoxic stress. The prototypes of the current generation, resveratrol and honokiol as shown in fig. 1, have been found; however, because of the suboptimal care they provided, patients have encountered sluggish healing and negative effects. Interesting research has revealed how mitochondrial dysfunction is mostly a result of SIRT3 downregulation and results in oxidative stress via high ROS levels. Thus, a better understanding of SIRT3's mitochondrial activity in neurons may lead to creative therapeutic strategies for preventing and treating neurodegenerative diseases associated with mitochondrial dysfunction. As free radical scavengers in the current work, we have produced benzylidene-based hydroxy benzyl urea derivatives that show neuroprotective effects and a diminution in ROS, which can be used in the treatment of PD.

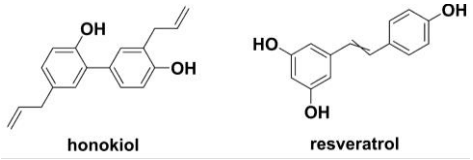

Fig. 1: Prototype current generations of selective SIRT3 activators

MATERIALS AND METHODS

Chemicals and reagents

The chemicals and reagents were purchased from the Carbino Innovative Chemical Interchange *Pvt. Ltd.* The thin-layer chromatography was made from silica gel G in the glass plate. The thin-layer chromatography was performed in the solvent system of 10% ethyl acetate and *n*-hexane. The spots obtained in the glass plates of thin-layer chromatography were visualized under a UV chamber. The melting point was obtained using the Veego VMP-I melting point apparatus. Further, the characterizations of the synthesized compounds were performed using Fourier transform infrared (FT-IR), Nuclear Magnetic Resonance (^{1}H-NMR and ^{13}C-NMR), and MS) where the data has been provided in the supplementary file.

In silico studies

Molecular docking

The molecular docking simulation studies were performed in the maestro of Schrodinger suite 2022 [8]. The designed ligands were converted to a three-dimensional state and the tool LigPrep module was used in the preparation by maintaining a pH of 7.2±7.0. The energy minimization was performed through the Epik module and

the OPLS3 force field was utilized [9]. The designed compounds have been displayed in Supplementary table 1. The RCSB, protein data bank https://www.rcsb.org/, was used in the extracting of the protein, PDB ID: 4fvt, which is a human SIRT3 confined to the Ac-ACS peptide and Carba-NAD+. The protein was prepared using the protein preparation wizard tool in Maestro, where the missing amino acids, water, and other hetero atoms were added and removed [10]. The grid box was prepared under the glide module in the receptor grid generation module [11]. The molecular docking of the designed compounds and prepared protein was performed under the Ligand docking module with a high degree of precision (XP) option to get accurate docking scores [12]. Among the designed compounds, the compound HBU-2 was found to have the highest docking score of -9.699 kcal/mol with an MM-GBSA score of -49.18. The designed compound HBU-2 showed interaction with PDB ID: 4fvt and 5 hydrogen bond interactions were observed with SER 321, THR 320, GLN 228, and ALA 146; these amino acids interactions showed the lipophilicity of the compounds, which could be considered to enhance the crossing of lipid membranes in the brain [13]. The hydrogen donor and hydrogen acceptor interactions were observed due to the hydroxyl group present in the designed compounds, whereas the hydrogen bond acceptor, the carbonyl group was found to produce hydrophobic interactions with the amino acids. Among the top hits, the compound HBU-4 was to have amino acid interactions with THR 320, SER 321, ASN 229, and PHE 180, these amino acids were both found to interact with polar and hydrophobic amino acids. The compound HBU-4 was to have a docking score of-9.020 kcal/mol. The hydrogen donor and hydrogen acceptor interactions were observed due to the hydroxyl group present in the designed compounds, whereas the hydrogen bond acceptor the carbonyl group, was found to produce hydrophobic interactions with the amino acids. Whereas, the hydrophobicity interactions were observed due to the carbon and hydrogen or aromatic ring present in the designed compounds. The standard molecule used for this study was resveratrol, which was found to have a docking score of-7.585 kcal/mol with an MM-GBSA score of-50.60. Here, Fig. 2. and fig. 3 illustrate the hydrophobicity and hydrogen bond acceptor regions within the protein and display the two-dimensional interactions between the designed ligand and amino acids of the protein. The designed compound HBU-1 to HBU-9 showed various interactions with the amino acid residues which has been displayed in Supplementary table 2.

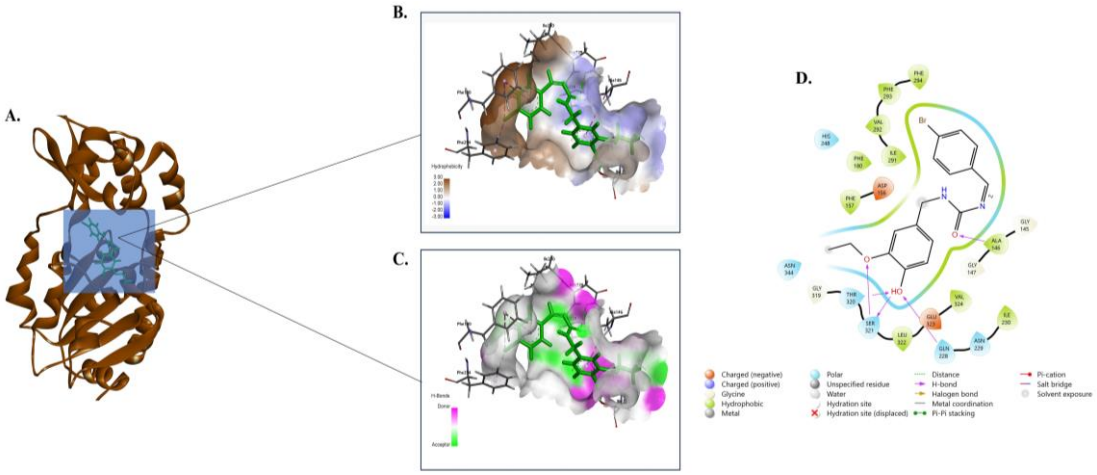

Fig. 2: 2D and 3D interactions for the compound HBU-2 and PDB ID: 4FVT. A. The Human SIRT3, PDB ID (4FVT) bound with the compound HBU-2. B. The compound HBU-2 (green color) with the amino acids interacting which are hydrophobic (brown color) C. The compound HBU-2 shows both hydrogen bond donor interaction (pink color) and hydrogen bond acceptor interaction (green color) with polar amino acid residue SD. The two-dimensional orientations of the designed compound HBU-2 with the sirtuin 3

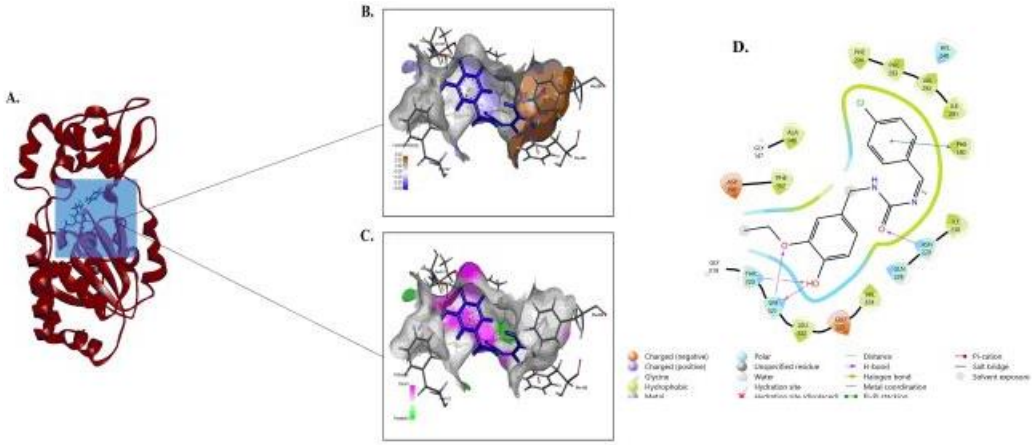

Fig. 3: 2D and 3D interactions for the compound HBU-4 and PDB ID: 4FVT. A. The Human SIRT3, PDB ID (4FVT) bound with the compound (Z)-1-(4-chlorobenzylidene)-3-(3-ethoxy-4-hydroxybenzyl) urea (HBU-4). B. The compound HBU-4 (blue color) with the amino acids interacting which are hydrophobic (brown color). C. The compound HBU-4 shows both hydrogen bond donor interaction (pink color) and hydrogen bond acceptor interaction (green color) with polar amino acid residues THR 320, SER 321, ASN 229, and hydrophobic amino residue PHE 180. D. The hydroxyl group of the phenyl ring was to be interacting with the SER 321, and THR 320. which are polar amino acid residues. The carbonyl group of the urea moiety which is an acceptor also visualized a polar amino residue interaction with ASN 229 amino acid residue followed by a pi-pi interaction with a hydrophobic amino acid residue PHE 180

Absorption, distribution, metabolism, and excretion (adme) studies

The designed compounds HBU-1 to HBU-10 (resveratrol) were investigated for ADME parameters [14]. The smaller molecules, which are more lipophilic have been found to penetrate through the tight junctions that lie in between endothelial cells in the brain [15]. The designed compound's molecular weight was observed in between 250-500 Daltons, which predicted the potency of enhancing oral absorption [16]. Qlog BB scores for the designed compounds HBU-1 to HBU 10 (resveratrol) predicted the penetration of the compound through the blood-brain barrier. Among the designed derivatives, the compound HBU-2 was found to have a Qlog BB of-1.03 and log p of 3.924, where it predicted the hydrophobicity and lipophilicity of the compound. The compound HBU-2 also predicted the number of hydrogen bond donors and acceptors which were in the required range. The compound HBU-4 also predicted the Qlog BB of-1.08, and log P of 3.785 with the hydrogen bond donor and acceptor in the required range. The higher log P determined the lipophilicity of the designed compounds [17]. The ADME scores for the designed compounds HBU-1 to HBU-10 (resveratrol) have been displayed in Supplementary table 3. The ADME scores predicted oral bioavailability, which enhances the absorption in the gastrointestinal tract where the metabolism of these compounds could also produce less risk of drug-drug interactions and toxicity [18].

Molecular mechanics with generalized born and surface area solvation (mm/gbsa)

The MM-GBSA studies for the designed compounds HBU-1 to HBU-10 (resveratrol) were performed to estimate the free energies produced between the compound and the PDB ID: 4FVT complex. The study helped in the screening of the top-hit compounds based on their bonding energies. The OPLS4 force field and VSGB solvation model used free energy (ΔG_{bind}) for the designed compounds that were predicted with the PDB ID: 4fvt active sites were calculated using the equation as follows:

$$\Delta G_{bind} = \Delta EMM + \Delta G_{solv} + \Delta GSA$$

Where ΔEMM was obtained by using OPLS4, which obtained the free energy between the designed compounds and PDB ID: 4fvt, the ΔG_{Solv} (GBSA solvation energy) was obtained as the solvation energy between the designed compounds and PDB ID: 4fvt. The surface energy difference between the designed compounds and the PDB ID: 4fvt was obtained, ΔGSA. The sum of these values was obtained in one single energy known as ΔG_{bind} [19]. Furthermore, the parameters $G_{covalent}$, $G_{couloumb}$, and G_{vdW} were determined using the Schrodinger suite 2022's MM-GBSA module. The compound HBU-2 was found to have the highest docking score of-9.699 kcal/mol with an MM-GBSA binding energy of-49.184 among all the designed derivatives, whereas having negative energy visualized favorable binding energy towards the protein [20]. The $\Delta G_{covalent}$ for the compound HBU-2 was found to be 8.56. The ΔG_{vdW} force for the compound and protein was found to be-39.16. Whereas the second-highest compound HBU-4 was found to have a MM-GBSA score of-51.37. The $\Delta G_{couloumb}$ for the compound HBU-4 was found to be-29.80. The ΔG_{vdW} for the designed ligand and protein was found to be-38.10. The scores obtained for the designed compounds have been displayed in fig. 4.

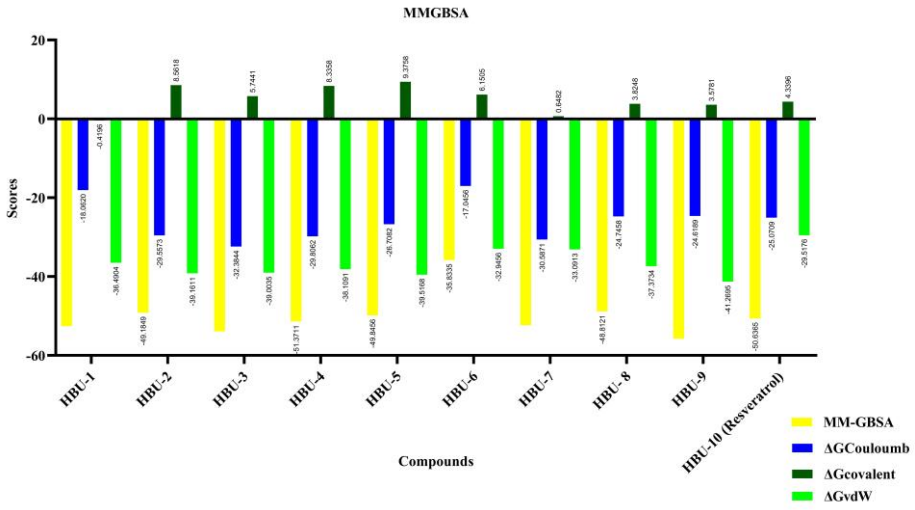

Fig. 4: The MMGBSA scores for the designed compounds HBU-1 to HBU-9

Molecular dynamics studies

The Desmond module in the Schrodinger suite 2022 was used to predict the stability of the compound/protein complex and to predict the various conformational changes of the selected compounds in the allosteric active sites of the protein (PDB ID: 4fvt) [21]. The stability study and various interactions between the compound and protein were studied at the time interval of 100 nanoseconds [22]. The parameters such as RMSD, RMSF, and hydrogen bond interactions were studied [23]. The compound and protein complex files were prepared using the OPLS4 force field in the system builder module [24]. The complex file was further minimized using the energy minimization tool in the maestro [25]. The molecular dynamic study tool was used to obtain the simulation and confirmational changes between the ligand and protein complex. The compound HBU-2 and the PDB ID: 4fvt stability was obtained with the help of protein-root mean square fluctuations (P-RMSF); where it showed a minimal interaction at 0.70 Å with the amino acid residue ALA 146, and stability was observed from 0.80 Å-0.60 Å with the amino acid residues ASP 156, SER 162, LEU 168, and PHE 193 (B). The ligand RMSF minimum fluctuation was observed at 2.68 Å, whereas the highest fluctuation was observed at 3.47 Å (C). Protein-ligand connections revealed essential amino-acid interactions such as hydrogen bonding, hydrophobic interactions, ionic bonds, and water bridges. The amino acids ILE 230, ASP 231, and PHE 157 formed strong hydrogen bond connections. Water bridge-based hydrogen interactions were observed with SER 49 and SER 159 amino acids. PHE 180, HIS 248, LEU 199, PHE 294, ARG 158, ILE 154, and ALA 146 were the hydrophobic interactions. Water bridge interactions were observed with the amino acid residues SER 162, PRO 176, GLU 177, and GLU 198, as illustrated in fig. 5.

General procedures for the synthesis of hbu-1 to hbu-9

According to Step 1, the 4-hydroxy-3-(methoxymethyl) benzaldehyde (1) (0.05 mmol) was added to hydrazine hydrate (2) (0.05 mmol), in the presence of ethanol and a few drops of glacial acetic acid was refluxed at 80 °C for 24 h. The reaction condition was monitored using thin-layer chromatography in a solvent

system of ethyl acetate and *n*-hexane (10%). The reaction mixture was precipitated at room temperature. The precipitates were filtered and recrystallized using ethanol and the desired compound 1-(3-ethoxy-4-hydroxybenzyl) urea (3) was obtained. In Step 2 the compound1-(3-ethoxy-4-hydroxybenzyl) urea (3) (0.05 mmol) was further treated with different aromatic substituted aldehydes (4) (0.05 mmol) in the presence of ethanol and glacial acetic acid, which was refluxed at 80 °C for 24 h. The reaction conditions were monitored using thin-layer chromatography. The precipitates were further filtered and dried at room temperature and the compounds HBU-1 to HBU-9 were obtained, as shown in fig. 6 [26-28].

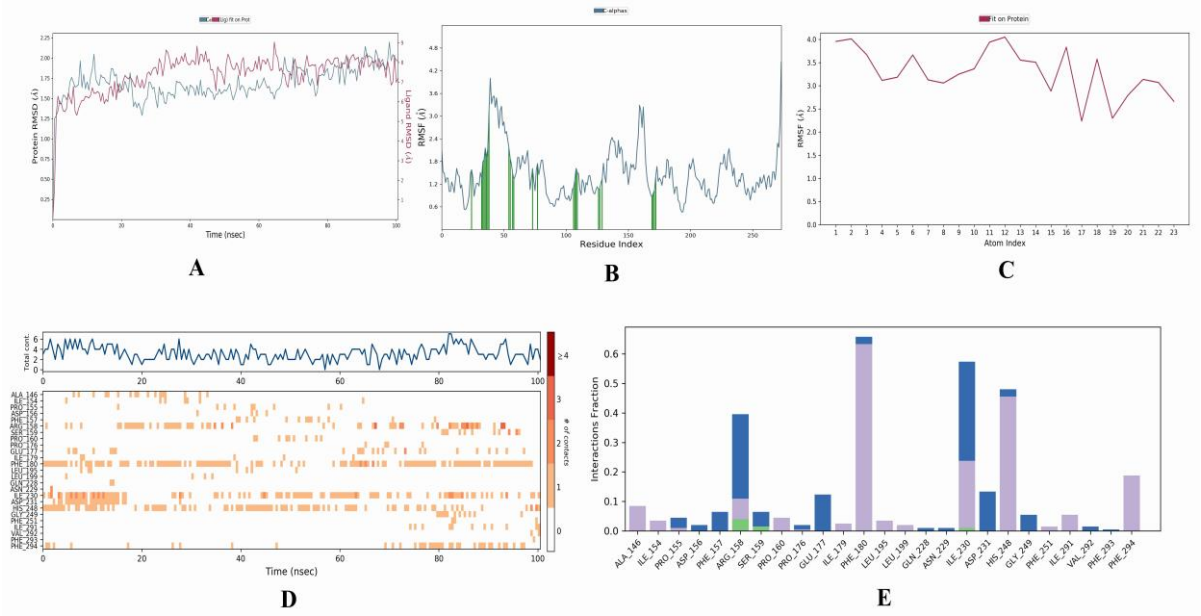

Fig. 5: Molecular dynamic simulation studies for the complex HBU-2/4FVT. A. Root Mean Square Deviations; RMSD of protein backbone atoms and HBU-2 derivatives. B. P-RMSF with the compound HBU-2 and SIRT3-based protein. C. Ligand root mean square fluctuations (L-RMSF). D. Ligand-protein two-dimensional summary interaction showing the highest energy involved with the amino acids. E. Protein-ligand contact visualizing hydrogen bond interactions

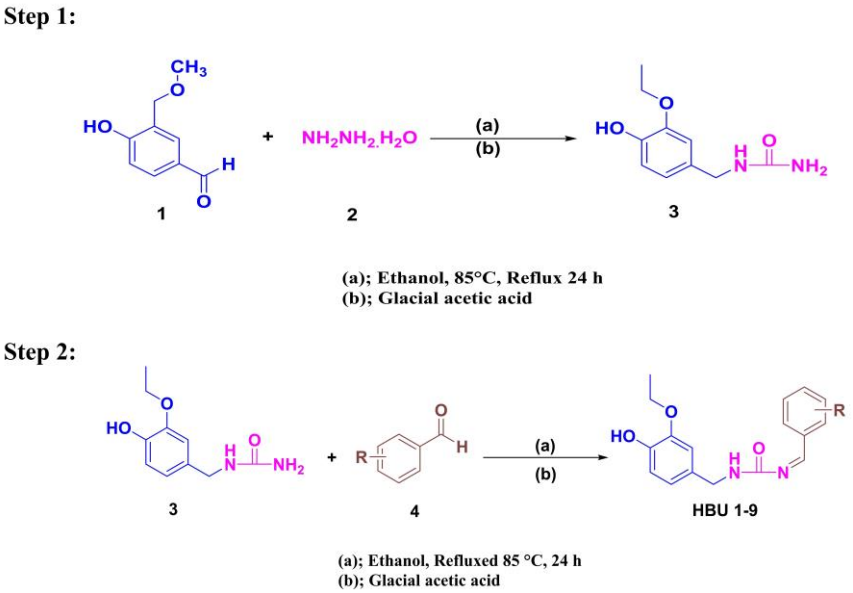

Fig. 6: Synthetic route for HBU-1 to HBU-9

(Z)-1-(3-chlorobenzylidene)-3-(3-ethoxy-4-hydroxybenzyl) urea (HBU-1)

The compound was prepared using the general procedure. Color: Yellow. Yeild: 72%; m. p. 145-146 °C; ^{1}H NMR (DMSO-d_6): δ =6.68 (2H, Ar-CH), 7.19-7.32 (3H, Ar-CH), 7.33-7.56 (5H, Ar-CH), 7.57-8.35 (5H, Ar-CH), 9.97 (1H, OH), 10.71 (1H, NH); ^{13}C NMR (DMSO-d_6): 56.80, 103.05, 114.91, 119.26, 122.09, 124.57, 125.00, 126.41, 127.11, 128.11, 129.35, 130.68, 131.34, 138.31, 140.86, 151.95; $C_{17}H_{17}BrN_2O_3$ (332.78) Observed m/z 335.

(Z)-1-(4-bromobenzylidene)-3-(3-ethoxy-4-hydroxybenzyl) urea (HBU-2)

The compound was prepared using the general procedure. Color: off-Yellow. Yeild: 66%; m. p. 155-158 °C; ^{1}H NMR (DMSO-d_6): δ= 6.69

(2H, Ar-CH), 7.01-7.19 (3H, Ar-CH), 7.22-7.55 (5H, Ar-CH), 7.80-8.35 (5H, Ar-CH), 9.97 (1H, OH), 10.71 (1H, NH); ^{13}C NMR (DMSO-$_{d6}$): 55.80, 104.05, 118.91, 120.26, 122.09, 123.57, 125.00, 126.41, 127.11, 128.11, 129.35, 130.68, 131.34, 138.31, 140.86, 151.95; $C_{17}H_{17}ClN_2O_3$ (377.24); Observed m/z 377.

(Z)-1-(3-ethoxy-4-hydroxybenzyl)-3-(4-methylbenzylidene) urea (HBU-3)

The compound was prepared using the general procedure. Color: off-White. Yeild: 70%; m. p. 120-122 ˚C; ^{1}H NMR (DMSO-$_{d6}$): δ= 2.33 (3H, CH_3), 6.79 (1H, Ar-CH), 7.11-7.20 (4H, Ar-CH), 7.24-7.77 (5H, Ar-CH), 7.88-8.40 (5H, Ar-CH), 9.80 (1H, OH), 10.71 (1H, NH); ^{13}C NMR (DMSO-$_{d6}$): 54.80, 102.05, 116.91, 121.26, 122.09, 123.57, 124.00, 126.41, 127.11, 128.11, 129.35, 130.68, 131.34, 138.31, 140.86, 151.95; $C_{18}H_{20}N_2O_3$ (312.37); Observed m/z 311.05.

(Z)-1-(4-chlorobenzylidene)-3-(3-ethoxy-4-hydroxybenzyl) urea (HBU-4)

The compound was prepared using the general procedure. Color: Yellow. Yeild: 75%; m. p. 158-160 ˚C; ^{1}H NMR (DMSO-$_{d6}$): δ= 6.40 (2H, Ar-CH), 7.11-7.20 (4H, Ar-CH), 7.24-7.77 (4H, Ar-CH), 7.88-8.40 (5H, Ar-CH), 9.80 (1H, OH), 10.71 (1H, NH); ^{13}C NMR (DMSO-$_{d6}$): 54.80, 102.05, 116.91, 121.26, 122.09, 123.57, 124.00, 126.41, 127.11, 128.11, 129.35, 130.68, 131.34, 138.31, 140.86, 151.95; $C_{17}H_{17}ClN_2O_3$ (332.78);); Observed m/z 336.05.

(Z)-1-(3-ethoxy-4-hydroxybenzyl)-3-(4-fluorobenzylidene) urea (HBU-5)

The compound was prepared using the general procedure. Color: White. Yeild: 68%; m. p. 132-134 ˚C; ^{1}H NMR (DMSO-$_{d6}$): δ= 6.39 (2H, Ar-CH), 7.04-7.32 (4H, Ar-CH), 7.36-7.77 (4H, Ar-CH), 7.88-8.40 (5H, Ar-CH), 9.80 (1H, OH), 10.71 (1H, NH); ^{13}C NMR (DMSO-$_{d6}$): 54.80, 102.05, 116.91, 121.26, 122.09, 123.57, 124.00, 126.41, 127.11, 128.11, 129.35, 130.68, 131.34, 138.31, 140.86, 151.95; $C_{17}H_{17}FN_2O_3$ (316.33); Observed m/z 315.00.

(Z)-1-(2,3-dichlorobenzylidene)-3-(3-ethoxy-4-hydroxybenzyl) urea (HBU-6)

The compound was prepared using the general procedure. Color: Yellow. Yeild: 74%; m. p. 145-147 ˚C; ^{1}H NMR (DMSO-$_{d6}$): δ= 6.55 (2H, Ar-CH), 7.10-7.32 (3H, Ar-CH), 7.28-7.75 (4H, Ar-CH), 7.80-8.40 (5H, Ar-CH), 9.80 (1H, OH), 10.71 (1H, NH); ^{13}C NMR (DMSO-$_{d6}$): 54.80, 102.05, 116.91, 121.26, 122.09, 123.57, 124.00, 126.41, 127.11, 128.11, 129.35, 130.68, 131.34, 138.31, 140.86, 151.95; $C_{17}H_{16}Cl_2N_2O_3$ (367.23); Observed m/z 366.20.

(Z)-1-(2,4-dichlorobenzylidene)-3-(3-ethoxy-4-hydroxybenzyl) urea (HBU-7)

The compound was prepared using the general procedure. Color: Yellow. Yeild: 70%; m. p. 144-145˚C; ^{1}H NMR (DMSO-$_{d6}$): δ= 6.45 (2H, Ar-CH), 7.10-7.32 (3H, Ar-CH), 7.28-7.75 (4H, Ar-CH), 7.80-8.40 (5H, Ar-CH), 9.80 (1H, OH), 10.71 (1H, NH); ^{13}C NMR (DMSO-$_{d6}$): 54.80, 102.05, 116.91, 121.26, 122.09, 123.57, 124.00, 126.41, 127.11, 128.11, 129.35, 130.68, 131.34, 138.31, 140.86, 151.95; $C_{17}H_{16}Cl_2N_2O_3$ (367.23); Observed m/z 367.10.

(Z)-1-benzylidene-3-(3-ethoxy-4-hydroxybenzyl) urea (HBU-8)

The compound was prepared using the general procedure. Color: Yellow. Yeild: 60%; m. p. 114-116˚C; ^{1}H NMR (DMSO-$_{d6}$): δ= 6.45 (3H, Ar-CH), 7.10-7.32 (3H, Ar-CH), 7.28-7.75 (4H, Ar-CH), 7.80-8.40 (5H, Ar-CH), 9.80 (1H, OH), 10.71 (1H, NH); ^{13}C NMR (DMSO-$_{d6}$): 54.80, 102.05, 116.91, 121.26, 122.09, 123.57, 124.00, 126.41, 127.11, 128.11, 129.35, 130.68, 131.34, 138.31, 140.86, 151.95; $C_{17}H_{16}Cl_2N_2O_3$ (298.34); Observed m/z 301.05.

(Z)-1-(4-(dimethylamino) benzylidene)-3-(3-ethoxy-4-hydroxybenzyl) urea (HBU-9)

The compound was prepared using the general procedure. Color: Off-White. Yeild: 66%; m. p. 120-122˚C; ^{1}H NMR (DMSO-$_{d6}$): δ= 2.44 (3H, CH_3), 6.45 (4H, Ar-CH), 7.10-7.32 (4H, Ar-CH), 7.28-7.75 (5H, Ar-CH), 7.80-8.40 (5H, Ar-CH), 9.80 (1H, OH), 10.71 (1H, NH); ^{13}C NMR (DMSO-$_{d6}$): 54.80, 102.05, 116.91, 121.26, 122.09, 123.57, 124.00, 126.41, 127.11, 128.11, 129.35, 130.68, 131.34, 138.31, 140.86, 151.95; $C_{19}H_{23}N_2O_3$(341.41); Observed m/z 341.95.

Biological evaluation

Neurotoxicity studies of the designed and synthesized compounds

The SH-SY5Y neuroblastoma cell lines were used in the determination of the cytotoxicity of the synthesized compounds [29]. The cultured cell group and the control group (untreated) exhibited a % cell viability of 100%. The cell lines were treated in the sample concentrations of 500 µg/ml, 250 µg/ml, and 125 µg/ml to identify the toxicity dose of the synthesized compounds. The cytotoxicity studies were performed for all the synthesized compounds, whereas the compound HBU-2 exhibited a % cell viability of 66.26%, 88.05%, and 91.22% at a sample concentration of 500, 250, and 125 µg/ml. The lowest toxicity was observed at the minimal concentration of the sample at 125 µg/ml. Whereas the compound HBU-4 exhibited a % cell viability of 86.13, 88.76, and 90.42% at a sample concentration of 500, 250, and 125 µg/ml. The % of the total variation was found to be 94.40, indicating a p-value of 0.0145. The two-way ANOVA ordinary alpha value for HBU-1 was found to be 0.05. The 95% confidence interval (CI) value was obtained between 15.73 and 50.37, indicating a significance value less than 0.05, indicating a significant (*) value. The % of the total variation was found to be 98.51, indicating a p-value of 0.05. The two-way ANOVA ordinary alpha value for HBU-3 was found to be 0.05. The 95 % CI value was obtained between 23.85 and 40.98, indicating a significance value less than 0.05, indicating a significant (*) value. The % of the total variation was found to be 98.70, indicating a p-value of 0.04. The two-way ANOVA ordinary alpha value for HBU-6 was found to be 0.05. The 95 % CI value was obtained between 19.30 and 31.95, indicating a significance value less than 0.05, indicating a significant (*) value. The % of the total variation was found to be 98.00, indicating a p-value of 0.03. The two-way ANOVA ordinary alpha value for HBU-7 was found to be 0.05. The 95 % CI value was obtained between 23.69 and 38.85, indicating a significance value less than 0.05, indicating a significant (*) value. The % of the total variation was found to be 98.00, indicating a p-value of 0.05. The two-way ANOVA ordinary alpha value for HBU-8 was found to be 0.05. The 95 % CI value was obtained between 14.99 and 35.41, indicating a significance value less than 0.05, indicating a significant (*) value. The % of the total variation was found to be 98.00, indicating a p-value of 0.02. The two-way ANOVA ordinary alpha value for HBU-8 was found to be 0.05. The 95 % CI value was obtained between 11.18 and 61.38, indicating a significance value less than 0.05, indicating a significant (*) value. The hypothesis proposed a major significance (*) p-value, where the variables were found to fail the null hypothesis, and all the variables were statistically found to be significant [30, 31]. The two-way ANOVA ordinary alpha value for HBU-2 was found to be 0.05. The 95 % CI value was obtained between 32.04 and 50.06, indicating a significance value of less than 0.004, indicating a significant (**) value. The two-way ANOVA ordinary alpha value for HBU-4 was found to be 0.05. The 95 % CI value was obtained between 29.07 and 40.88, indicating a significance value of less than 0.003, indicating a significant (**) value, as shown in fig. 7.

Neuroprotection of HBU-2 and HBU-4

Recent studies have claimed how 1-methyl-4-phenylpyridinium (MPP^+)has been used in the induction of dopaminergic cell death [32]. In this study, 0.5 mmol of $MPP^+$was induced to the SHSY5Y cell line to cause toxicity to the cells at 20˚C, and the treatment was provided by the top % cell viability compounds HBU-2, and HBU-4 with a dose selectivity of 125 µg/ml. The control group (untreated) showed high cell survival in fold change (cell count), and lactate dehydrogenase (LDH) cells showed no cytotoxicity. The induction of MPP^+ decreased the cell count to minimal fold change and % cytotoxicity. The treatment group with HBU-2 and HBU-4 improved the overall cell survival growth in both cell count and LDH assay. The increased LDH count results in toxicity to the cells [33]. The synthesized compounds HBU-2, and HBU-4 were able to control the further toxicity in the cell lines, shown in fig. 8.

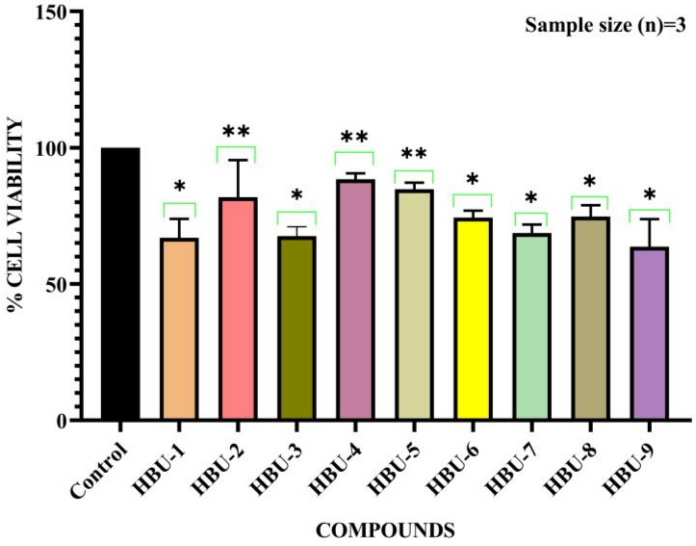

Fig. 7: Two-way ANOVA analysis. HBU-2, HBU-4, and HBU-5 with most significance compared to other compounds. (***) p<0.001-Very strong significance against the null hypothesis; (**) p<0.011-Strong significance against the null hypothesis; (*) p<0.05-Good significance against the null hypothesis; (no significant) p>0.01-No significance against the null hypothesis

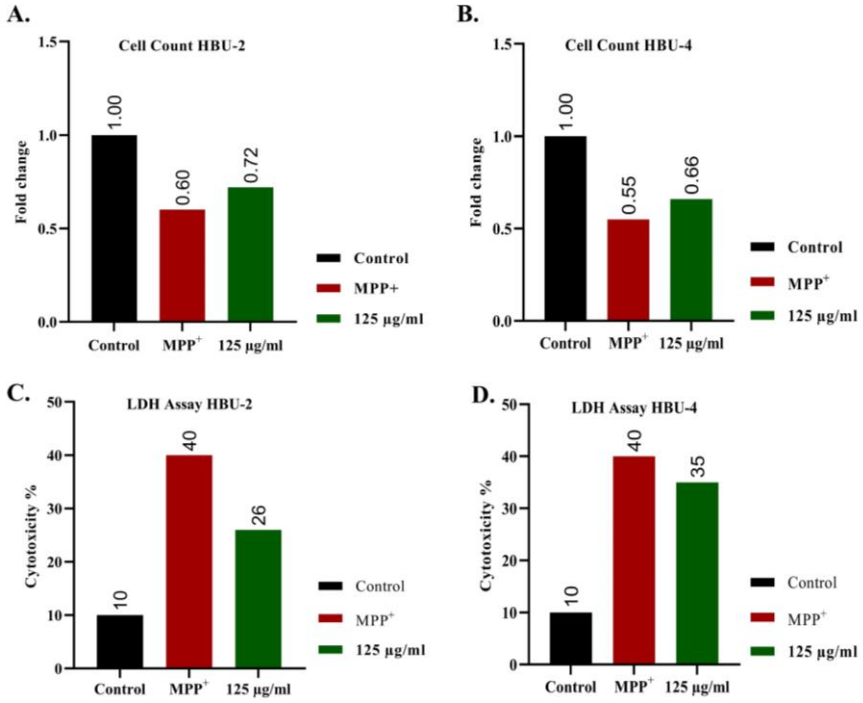

Fig. 8: The synthesized compounds were studied for neurotoxicity via the cell count and LDH assay. A. The control (untreated cells) was found to exhibit no decrease in the cell count, whereas the induced MPP+ showed a decrease in cell count to 0.60-fold change, and the treatment group HBU-2 at 125 µg/ml increased the cell count to 0.72-fold change. B. The control (untreated cells) was found to exhibit no decrease in the cell count, whereas the induced MPP+ showed a decrease in cell count to 0.55-fold change, and the treatment group at 125 µg/ml increased the cell count to 0.66-fold change. C. The LDH assay in the control (untreated) group exhibited no cytotoxicity. In contrast, at inducing MPP+, 40 % of the cytotoxicity was observed, and after treating it with the HBU-2 the LDH level was reduced to 26% at 125 µg/ml. D. The LDH assay in the control (untreated) group exhibited no cytotoxicity, whereas at inducing MPP+40 % of the cytotoxicity was observed, and after treating it with the HBU-4 the LDH level was reduced to 35 % at 125 µg/ml

Treating the ros level by HBU-2 and HBU-4

Normal ROS levels in the cell participate in cellular activity and cellular signaling [34]. An increased % of ROS results in the formation of oxidative stress in the cells, which results in cellular deaths [35]. The SHSY5Y neuroblastoma cell lines were studied with the control (untreated), and treated groups with the compound HBU-2, and HBU-4 at different concentrations of 500 µg/ml, 250 µg/ml, 125 µg/ml. The 0.5 nM of MPP^+ increased the ROS level in the cells, whereas the treated cells with HBU-2, and HBU-4 were found to decrease the ROS % in the cells. The ROS % was brought down in the treated groups by HBU-2, and HBU-4. The study showed that the compound HBU-2 was more potent as compared to the HBU-4 compound, which reduced the ROS level in the cells shown in fig. 9.

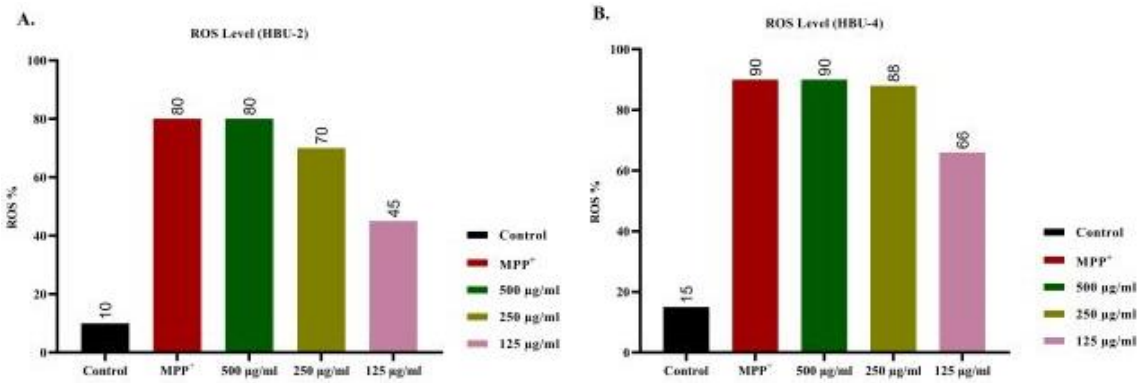

Fig. 9: ROS Level study compared to the HBU-2, and HBU-4 compounds. A. The ROS % in the control group was found to be 10 %, where the MPP+ continuously increased the ROS % up to 80 %; by treating the cells at 125 µg/ml the ROS % was found to be decreased to 45 % by the compound HBU-2. B. The ROS % in the control group was found to be 10 %, where the MPP+continuously increased the ROS % up to 80 %, by treating the cells at 125 µg/ml the ROS % was found to be decreased to 66 % by the compound HBU-4

CONCLUSION

In this study, benzylidene-based hydroxy benzyl urea derivatives were found to be counteracting free radicals and they downregulated the ROS level, which resulted in less oxidative stress. The compounds HBU-2, and HBU-4 were found to have the highest docking/binding affinity towards the selected PDB ID: 4fvt (Sirtuin 3) among all the nine derivatives. The binding affinity for all the compounds was obtained in the range of-7.00 to-9.699 kcal/mol. The compound HBU-2 had a binding affinity of-9.699 kcal/mol, which generally showed capable protein interactions. The amino acids THR 320, SER 321, GLN 228, and ALA 146 which are hydrophobic and polar amino acids could potentiate the proper functioning. The *in vitro* study on SHSY-5Y cell lines was done. The cells were treated with higher concentrations (500 µg/ml, 250 µg/ml, and 125 µg/ml). The control (untreated) group and treatment (MPP+/compounds) showed outstanding changes in the downregulation of ROS levels and oxidative stress. The cytotoxicity studies showed that HBU-2 and HBU-4 were found to have little harm in the cells with a % cell survival of 91.22 % and 90.42 % at a concentration of 125 µg/ml. The neuroprotection study showed how the MPP+generation in the cell raised the LDH counts and lowered the cell counts, while the treatment of the cells with the HBU-2 and HBU-4 repaired the MPP+damages in the cells. In the antioxidant trial for all the synthesized derivatives, the substance HBU-2 was proven to have the best antioxidant value of 45.05 at a minimum concentration of 125 µg/ml. The cells treated with the MPP+raised the ROS level to 80 % and 90 %, where the ROS levels were dropped to 45 % and 66 % at 250 µg/ml, and 125 µg/ml concentrations. The ROS effect and oxidative stress have been widely involved in brain death and cellular mortality. The antioxidants are frequently utilized in counteracting the effect of rising ROS levels. Overall, our results showed that the predicted and synthesized benzylidene-based hydroxy benzyl urea derivatives can be good free radical scavengers and may become an optional therapeutic option in treating PD.

ACKNOWLEDGMENT

"We acknowledge the generous research infrastructure and support from JSS College of Pharmacy, JSS Academy of Higher Education and Research, Rocklands, Ooty, The Nilgiris, Tamilnadu, India".

AUTHORS CONTRIBUTIONS

JC has supervised the study, ATK has performed the synthetic and characterization study, KP has performed the *in silico* studies, JM, has performed the *in vitro studies*, FS has written the manuscript, GS has revised the manuscript.

CONFLICT OF INTERESTS

Declared none

REFERENCES

1. Krishnamurthy G, Deepti Roy L, Kumar J, Gour P, Arland SE, Rehman N. Design, preparation, and *in silico* study of novel curcumin-biphenyl carbonitrile conjugate as novel anticancer drug molecules. Int J App Pharm. 2023;15(4):143-59. doi: 10.22159/ijap.2023v15i4.45811.
2. Subramanian G, Chand J, Jupudi S, Prudviraj P. Synthesis and biological evaluation of the selected naphthalene substituted azetidinone derivatives targeting Parkinson's disease. Ind J Pharm Edu Res. 2023;57(2):552-58. doi: 10.5530/ijper.57.2.68.
3. Rohini D, Vijayalakshmi K. Sesamol antagonizes rotenone-induced cell death in SH-SY5Y neuronal cells. Int J Pharm Pharm Sci. 2016;8(12):72. doi: 10.22159/ijpps.2016v8i12.14529.
4. Mohan R, Kayalvizhi RR, Ramanathan R, Shanmugam J, RA. Impact of caloric vestibular stimulation on co-ordination in Parkinson disease induced mice. Int J Pharm Pharm Sci. 2022;14(10):46-9. doi: 10.22159/ijpps.2022v14i10.45523.
5. Dorszewska J, Kowalska M, Prendecki M, Piekut T, Kozłowska J, Kozubski W. Oxidative stress factors in Parkinson's disease. Neural Regen Res. 2021;16(7):1383-91. doi: 10.4103/1673-5374.300980, PMID 33318422.
6. Sawa K, Uematsu T, Korenaga Y, Hirasawa R, Kikuchi M, Murata K. Krebs cycle intermediates protective against oxidative stress by modulating the level of reactive oxygen species in neuronal HT22 cells. Antioxidants (Basel). 2017;6(1):21. doi: 10.3390/antiox6010021, PMID 28300753.
7. Shen Y, Wu Q, Shi J, Zhou S. Regulation of SIRT3 on mitochondrial functions and oxidative stress in Parkinson's disease. Biomed Pharmacother. 2020;132:110928. doi: 10.1016/j.biopha.2020.110928, PMID 33128944.
8. Jha V, Dhamapurkar V, Thakur K, Kaur N, Patel R, Devkar S. *In silico* prediction of potential inhibitors for the M2 protein of influenza a virus using molecular docking studies. Asian J Pharm Clin Res. 2022;15(8):100-8. doi: 10.22159/ajpcr.2022.v15i8.44608.
9. Badavath VN, Sinha BN, Jayaprakash VE. Design, *in silico* docking and predictive ADME properties of novel pyrazoline derivatives with selective human MAO inhibitory activity. Int J Pharm Pharm Sci. 2015;7:277-82.
10. Boulaamane Y, Ibrahim MAA, Britel MR, Maurady A. *In silico* studies of natural product-like caffeine derivatives as potential MAO-B inhibitors/AA2AR antagonists for the treatment of Parkinson's disease. J Integr Bioinform. 2022;19(4):20210027. doi: 10.1515/jib-2021-0027, PMID 36112816.
11. Szczepankiewicz BG, Dai H, Koppetsch KJ, Qian D, Jiang F, Mao C. Synthesis of carba-NAD and the structures of its ternary complexes with SIRT3 and SIRT5. J Org Chem. 2012;77(17):7319-29. doi: 10.1021/jo301067e, PMID 22849721.
12. Fan G, Chen S, Tao Z, Zhang H, Yu R. A novel small positive allosteric modulator of neuropeptide receptor PAC1-R exerts neuroprotective effects in MPTP mouse Parkinson's disease model. Acta Biochim Biophys Sin (Shanghai). 2022;54(9):1349-64. doi: 10.3724/abbs.2022126, PMID 36082935.
13. Subramanian G, Jupudi S, Chand J, Zubair Baba M. Network pharmacology approach and molecular docking prediction to

investigate the possible mechanism of benzylidene derivatives against scavenging reactive oxygen species via sirtuin 3 Parkinson's disease. Biointerface Res J Appl Chem. 2024;14(2):48.

14. Mathew GE, Oh JM, Mohan K, Tengli A, Mathew B, Kim H. Development of methylthiosemicarbazones as new reversible monoamine oxidase-b inhibitors for the treatment of Parkinson's disease. J Biomol Struct Dyn. 2021;39(13):4786-794. doi: 10.1080/07391102.2020.1782266, PMID 32588753.
15. Kealy J, Greene C, Campbell M. Blood-brain barrier regulation in psychiatric disorders. Neurosci Lett. 2020;726:133664. doi: 10.1016/j.neulet.2018.06.033, PMID 29966749.
16. Zubair Baba M, Subramanian G, Chand J, Wahedi U, Varakumar P, Jayanthi K. Investigation of scutellaria baicalensis for potential neuroprotective effect on the treatment of Parkinson's disease. Biointerface Res Appl Chem. 2024;14(2):27.
17. Morak Młodawska B, Jelen M. Lipophilicity and pharmacokinetic properties of new anticancer dipyridothiazine with 1,2,3-triazole substituents. Molecules. 2022;27(4):1253. doi: 10.3390/molecules27041253, PMID 35209047.
18. Peng Y, Cheng Z, Xie F. Evaluation of pharmacokinetic drug-drug interactions: a review of the mechanisms, *in vitro* and *in silico* approaches. Metabolites. 2021;11(2):75. doi: 10.3390/metabo11020075, PMID 33513941.
19. Dasmahapatra U, Kumar CK, Das S, Subramanian PT, Murali P, Isaac AE. In-silico molecular modelling, MM/GBSA binding free energy and molecular dynamics simulation study of novel pyrido fused imidazo[4,5-c]quinolines as potential anti-tumor agents. Front Chem. 2022;10:991369. doi: 10.3389/fchem.2022.991369, PMID 36247684.
20. Taylor M, Ho J. MM/GBSA prediction of relative binding affinities of carbonic anhydrase inhibitors: effect of atomic charges and comparison with Autodock4Zn. J Comput Aided Mol Des. 2023;37(4):167-82. doi: 10.1007/s10822-023-00499-0, PMID 36930332.
21. Ranade SD, Alegaon SG, Venkatasubramanian U, Soundarya Priya A, Kavalapure RS, Chand J. Design, synthesis, molecular dynamics simulation, MM/GBSA studies and kinesin spindle protein inhibitory evaluation of some 4-aminoquinoline hybrids. Comput Biol Chem. 2023;105:107881. doi: 10.1016/j.compbiolchem.2023.107881, PMID 37257398.
22. Subramanian G, Prasad K, Chand J, Amarjith TK, Shanish AA. In-silico, synthesis, characterization, and *in vitro* studies on benzylidene-based 2-chloroquinolin derivatives as free radical scavengers in Parkinson's disease. Drug Res. 2024;74(2):67-76. doi: 10.1055/a-2231-1311, PMID 38346682.
23. Lokhande KB, Ballav S, Yadav RS, Swamy KV, Basu S. Probing intermolecular interactions and binding stability of kaempferol, quercetin and resveratrol derivatives with PPAR-γ: docking, molecular dynamics and MM/GBSA approach to reveal potent PPAR- γ agonist against cancer. J Biomol Struct Dyn. 2022;40(3):971-81. doi: 10.1080/07391102.2020.1820380, PMID 32954977.
24. Kurki M, Poso A, Bartos P, Miettinen MS. Structure of POPC lipid bilayers in OPLS3e force field. J Chem Inf Model. 2022;62(24):6462-474. doi: 10.1021/acs.jcim.2c00395, PMID 36044537.
25. Elekofehinti OO, Iwaloye O, Josiah SS, Lawal AO, Akinjiyan MO, Ariyo EO. Molecular docking studies, molecular dynamics and ADME/tox reveal therapeutic potentials of STOCK1N-69160 against papain-like protease of SARS-CoV-2. Mol Divers. 2021;25(3):1761-73. doi: 10.1007/s11030-020-10151-w, PMID 33201386.
26. Silverberg LJ, Coyle DJ, Cannon KC, Mathers RT, Richards JA, Tierney J. Azeotropic preparation of a C-phenyl N-aryl imine: an introductory undergraduate organic chemistry laboratory experiment. J Chem Educ. 2016;93(5):941-44. doi: 10.1021/acs.jchemed.6b00056.
27. Hamama WS, Ibrahim ME, Gooda AA, Zoorob HH. Recent advances in the chemistry of 2-chloroquinoline-3-carbaldehyde and related analogs. RSC Adv. 2018;8(16):8484-515. doi: 10.1039/c7ra11537g, PMID 35539824.
28. Ghandi M, Efteghar I, Abbasi A. One-pot synthesis of quinoline-fused [1,4]thiazepines via the tandem Ugi/post-Ugi reactions. J Iran Chem Soc. 2019;16(2):325-32. doi: 10.1007/s13738-018-1511-z.
29. Khanal P, Patil BM. *In vitro* and *in silico* anti-oxidant, cytotoxicity and biological activities of ficus benghalensis and duranta repens. Chin Herb Med. 2020;12(4):406-13. doi: 10.1016/j.chmed.2020.02.004, PMID 36120176.
30. Andrade C. The P value and statistical significance: misunderstandings, explanations, challenges, and alternatives. Indian J Psychol Med. 2019;41(3):210-15. doi: 10.4103/IJPSYM.IJPSYM_193_19, PMID 31142921.
31. Silva S, Marto J, Gonçalves L, Almeida AJ, Vale N. Formulation, characterization and evaluation against SH-SY5Y cells of new tacrine and tacrine-MAP loaded with lipid nanoparticles. Nanomaterials (Basel). 2020;10(10):2089. doi: 10.3390/nano10102089, PMID 33096919.
32. Enogieru AB, Haylett W, Hiss D, Ekpo O. Inhibition of γH2AX, COX-2 and regulation of antioxidant enzymes in MPP+-exposed SH-SY5Y cells pre-treated with rutin. Metab Brain Dis. 2021;36(7):2119-30. doi: 10.1007/s11011-021-00746-z, PMID 33978902.
33. Strother L, Miles GB, Holiday AR, Cheng Y, Doherty GH. Long-term culture of SH-SY5Y neuroblastoma cells in the absence of neurotrophins: a novel model of neuronal ageing. J Neurosci Methods. 2021;362:109301. doi: 10.1016/j.jneumeth.2021.109301, PMID 34343572.
34. Lennicke C, Cocheme HM. Redox metabolism: ROS as specific molecular regulators of cell signaling and function. Mol Cell. 2021;81(18):3691-707. doi: 10.1016/j.molcel.2021.08.018, PMID 34547234.
35. Patil PP, Kumar P, Khanal P, Patil VS, Darasaguppe HR, Bhandare VV. Computational and experimental pharmacology to decode the efficacy of Theobroma cacao L. against doxorubicin-induced organ toxicity in EAC-mediated solid tumor-induced mice. Front Pharmacol. 2023;14:1174867. doi: 10.3389/fphar.2023.1174867, PMID 37324470.